2019 IEEE MTT-S International Conference on Numerical Electromagnetic and Multiphysics Modeling and Optimization (NEMO)

Volume Rooftop Basis Functions in Shielded Layered Media

James C. Rautio
Sonnet Software, Inc.
Syracuse, NY USA
rautio@sonnetsoftware.com

Matthew Thelen
Sonnet Software, Inc.
Syracuse, NY USA

***Abstract*—Infinitely thin planar circuits are often represented with rooftop basis functions. These basis functions use a sheet of surface current over the area of a subsection and are overlapped to generate a piece-wise linear representation of the actual surface current. This paper extends rooftop functions to volume current. Volume current rooftop subsections are overlapped in a similar fashion to represent the volume current flowing in a thick conductor. Layered media enclosed in a rectangular shielding conductor is assumed. This allows fast and numerically exact evaluation of the Green's function with the resulting method of moments reaction integrals evaluated analytically, rather than numerically. Use of volume rooftops results in faster high accuracy analysis of planar circuits composed of thick metal, especially for lines with a high aspect ratio cross-section.**

Keywords—basis function, boundary element method, electromagnetic, Galerkin, layered dielectric, method of moments, planar circuit, rooftop.

I. Introduction

The method of moments [1] (also sometimes called the boundary element method) is often used to analyze planar circuits on layered dielectric. Extensive use is seen in unshielded environments, usually for planar antenna analysis or for scattering from arbitrary objects, for example [2]–[5]. In fact [2] already uses a volume rooftop basis function for polarization current. However, evaluation of the Green's function in an unshielded, i.e., laterally open environment is numerically intense and subject to approximations in order to increase the speed of analysis, as in [5], for example.

Use of infinitely thin, surface current based rooftop functions [6] in shielded (i.e., inside a conducting box) layered media is described in [7]. Here we extend the overlapping infinitely thin surface rooftops to overlapping volume rooftops that span the volume of a thick planar conductor. Unlike the unshielded case, the Green's function can be quickly evaluated (using the FFT algorithm) to full numerical accuracy. In addition the required method of moments reaction integrals are evaluated analytically, also to full numerical accuracy. This makes these basis functions ideal for high accuracy analysis, especially in extreme cases such as at very high frequency, with extreme dimensions (large or small) or extreme material parameters.

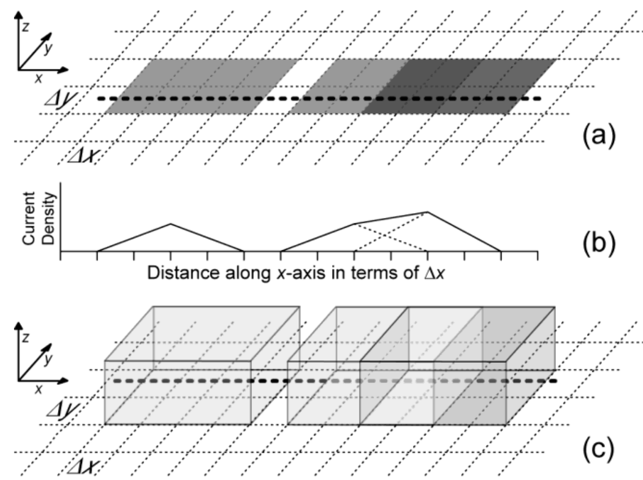

Fig. 1. Infinitely thin rooftop footprints cover a cell grid in (a). The x-directed surface current (A/m) along the thick dashed line is shown in (b) and is the same everywhrere across the y-width of the subsection. On the right side, two overlapping rooftops allow a piece-wise linear representation of the current. Volume rooftops, (c), have the same current density (b) everywhere across their y-z cross-sections along the thick dotted line, only now (b) dipicts a volume current (A/m^2). Two subsections overlap in the right side of (c) in a manner analogous to the right side of (a).

II. Problem Definition

Fig. 1a shows a cell grid (dotted lines). Infinitely thin subsections with x-directed current are illustrated. Each x-directed subsection is $4\Delta x$ long by $2\Delta y$ wide while y-directed subsections (not illustrated) are $2\Delta x$ wide and $4\Delta y$ long. A surface current based rooftop covers eight cells, as outlined with the shaded rectangle. Current flows along the length of rooftop subsections. The assumed surface current density (A/m) along the dashed line is shown in Fig. 1b. The current density is the same no matter where the dashed line is positioned across the y-width of the subsection. Note the ramp-up and then the ramp-down in the left hand portion of Fig. 1b. When two rooftops are overlapped, as in the right hand portion of Fig. 1a, we have the current distribution shown in the right hand portion of Fig. 1b. Thus overlapping rooftops yield a piece-wise linear representation of the current flowing on the surface of infinitely thin conductor.

Fig. 1c. shows volume rooftops. The volume current flowing along the dashed line in the volume rooftop is also

978-1-5386-9516-6/19/$31.00 ©2019 IEEE

shown in Fig. 1b (consider Fig. 1b to now be plotted in A/m^2). Likewise, this current distribution is the same no matter where the dashed line is positioned within the *y-z* cross-section of the rooftop. As with the surface rooftops of Fig. 1a, the overlapping volume rooftops on the right hand side of Fig. 1c yield a piece-wise linear representation of the current flowing in a thick conductor.

For a complete solution, the conductor of a given circuit is meshed with rooftop subsections twice, once for *x*-directed current and a second time for *y*-directed current. The same underlying cell grid is used for both meshings.

Our task is to determine the required Galerkin reaction integrals to implement a method of moments solution for arbitrary thick planar circuits. In conceptual terms, this means evaluating the total voltage induced on one subsection due to current on another subsection.

III. Shielded Layered Green's Function

The Green's function for an infinitely thin sheet of current located at the interface between two layers of dielectric with perfectly conducting covers on top and bottom is derived, for example, in [7]. The *z*-axis is perpendicular and the dielectric interface is parallel to the covers.

For this work we weight and sum all *m*, *n* TE_z and TM_z rectangular waveguide modes formed by the sidewalls of the shielding box. These summations are indicated by using the generic index *i* to cover all modes We assume the top and bottom covers terminate the sidewall-waveguide and have a resistivities r_{iT} and r_{iB} (both of which, in general, are complex). We also assume that both dielectric layers have the same constitutive parameters, yielding identical wavenumbers and characteristic admittances, k_{iz} and Y_i. As in [7], the Y_i are the admittances of the standing wave modes, differing by a factor of *j* from the usual rectangular waveguide characteristic admittances. Placing the bottom cover at $z = 0$, the top cover at $z = h$, the interface between the two dielectric layers at z', and letting $\boldsymbol{u}_S$ be the unit vector of the direction of the transverse-to-*z* source current located at (x', y', z'), the Green's function for transverse electric field generated by transverse current is

$$G_t = -\sum_i \frac{g_T(z) g_B(z') [\boldsymbol{u}_S \cdot \boldsymbol{e}_{it}(x', y')]}{Y_i g_D} \boldsymbol{e}_{it}(x, y), \quad z \geq z' \quad (1)$$

$$G_t = -\sum_i \frac{g_T(z') g_B(z) [\boldsymbol{u}_S \cdot \boldsymbol{e}_{it}(x', y')]}{Y_i g_D} \boldsymbol{e}_{it}(x, y), \quad z \leq z' \quad (2)$$

where

$$g_B(u) = \sin(k_{iz} u) + r_{iB} \cos(k_{iz} u) \quad (3)$$

$$g_T(u) = \sin\big(k_{iz}(h-u)\big) + r_{iT} \cos\big(k_{iz}(h-u)\big) \quad (4)$$

$$g_D = (1 - r_{iB} r_{iT}) \sin(k_{iz} h) + (r_{iT} + r_{iB}) \cos(k_{iz} h). \quad (5)$$

The $\boldsymbol{e}_{it}$ are the transverse normalized rectangular waveguide mode vectors used in [7], from Marcuvitz [8].

Next, we multiply (1) and (2) by the volume rooftop current distribution with the bottom center of the subsection located at $(x_0, y_0, 0)$ and perform a volume integration over the primed coordinates. The thickness of the volume rooftop extends from $z = 0$ to $z = h$. The result is unexpectedly simple.

$$\boldsymbol{E}_{tVRF} = \sum_i \frac{C_{iS}(x_0, y_0)}{Y_i k_{iz}} \left(1 - \frac{g_T(z) + g_B(z)}{g_D}\right) \boldsymbol{e}_{it}(x, y) \quad (6)$$

The C_{iS} are the Fourier coefficients for the source subsection, which result from the Green's function integration.

$$C_{iRFX}(x_0, y_0) = F_T(\Delta x) F_R(\Delta y) \left[\boldsymbol{e}_{it}(x_0, y_0) \cdot \boldsymbol{u}_x\right] \quad (7)$$

$$C_{iRFY}(x_0, y_0) = F_R(\Delta x) F_T(\Delta y) \left[\boldsymbol{e}_{it}(x_0, y_0) \cdot \boldsymbol{u}_y\right] \quad (8)$$

$$F_R(\Delta x) = \begin{cases} \frac{2}{k_x} \sin(k_x \Delta x), & k_x \neq 0 \\ \Delta x, & k_x = 0 \end{cases} \quad (9)$$

$$F_T(\Delta x) = \begin{cases} \frac{1}{\Delta x k_x^2} (1 - \cos(k_x \Delta x)), & k_x \neq 0 \\ 2\Delta x, & k_x = 0 \end{cases} \quad (10)$$

The subscripts indicate the type of subsection. A RFX subscript indicates a rooftop with *x*-directed current, as in Fig. 1a and 1c. The current on a RFX subsection has a triangle function dependence in the direction of current flow (subscript *T*, above) and a rectangle (i.e., constant) current dependence across the width of the subsection (subscript *R*, above).

With the fields surrounding a volume rooftop determined by (6), we must evaluate what we call the 'volume voltage' on the field subsection. This is the volume integral of the electric field dotted with the basis function current distribution on the field subsection, in this case, another volume rooftop. This is the reaction integral required for our method of moments analysis. Since we are weighting the volume voltage integral with the field subsection basis function, this is a Galerkin version of the method of moments. The result is once more unexpectedly simple.

$$S = \sum_i \frac{C_{iF} C_{iS}}{Y_i k_{iz}^2} \left(k_{iz} h - \frac{2(1 - \cos(k_{iz} h)) + (r_{iT} + r_{iB}) \sin(k_{iz} h)}{g_D}\right) \quad (11)$$

The C_{iF} are the Fourier coefficients for the field subsection. Thus, (7)–(10) are evaluated at (x_1, y_1), the center of the field subsection. C_{iF} are the result of the volume voltage integration. The C_{iS} follow from (6), and are evaluated at (x_0, y_0), the center of the source subsection.

Because we are working in a shielded layered environment, this summation is evaluated rapidly and efficiently to full numerical precision using a single 2-D FFT. This single FFT provides any and all possible pair-wise couplings between any two given types of subsections located anywhere within the substrate.

IV. Preliminary Validation

We have implemented (11) in a commercial method of moments program [9] and compared results for a thick transmission line with a right angle bend. Correct results are determined by convergence analysis, where we repeatedly cut cell size by half and plot results. The EM software used has been demonstrated to converge asymptotically to the exact answer [10].

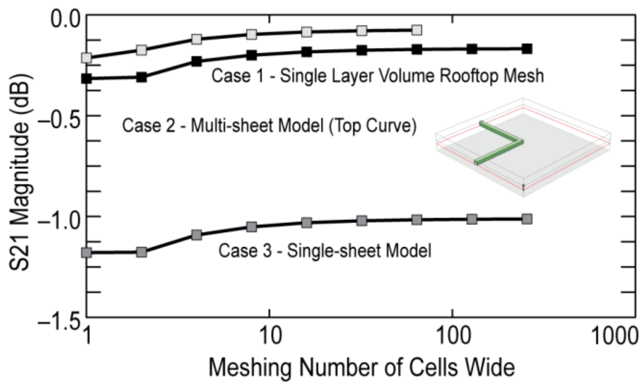

Fig. 2. Convergence analysis of a thick stripline with square cross-section. Case 1 uses a single layer of volume rooftop subsections. Case 2 (top curve) uses multiple infinitely thin sheets of current. Case 3 uses a single infinitely thin sheet of current. Results are plotted as cell size is reduced.

The subject transmission line cross-section is 0.254 mm square and is analyzed at 4.0 GHz. The transmission line is surrounded by homogenous and isotropic dielectric with ε_{rel} = 2.94. This stripline geometry has dielectric above the top conductor surface and below the bottom conductor surface 0.508 mm thick. There is a length of 3.81 mm of thick transmission line connecting both ends of the right angle bend to adjacent conducting sidewalls. The right angle bend is in the center of a square substrate 8.128 mm on a side. The effect of port discontinuities are removed. Port reference planes are set at the box walls.

We evaluated the line using 1) A single layer of the volume rooftop subsections described here, 2) Multiple infinitely thin sheets equally spaced and stacked one on top of another to simulate a thick conductor and 3) An infinitely thin one-sheet line. We divide the width of each line into an equal number, N, of subsections. As N increases, we realize an increasingly accurate representation of the current distribution on the top and bottom surfaces of the line. Simultaneously, we divide the thickness of the multi-sheet line, Case 2, into N+1 sheets. Case 1, which uses volume rooftops, is left at one subsection thick.

Fig. 2 shows the results. Notice that Case 3, the single sheet, infinitely thin line is, as expected, substantially different from both thick metal models. This confirms that this line geometry is sensitive to line thickness. Case 2, as N increases, is expected to converge asymptotically to the exact answer [10]. Case 1, using a single layer of volume rooftops is close to Case 2, but not identical. We expect the difference is due to a uniform representation of current on the side surfaces of the thick line of Case 1. Case 2, with multiple sheets, asymptotically approaches the exact current distribution on the sides of the line, but at the cost of substantially longer analysis time. In fact, N = 128 and 256 could not be analyzed with existing computer resources for Case 2.

To check the side current distribution hypothesis suggested in the above paragraph, we analyze an extreme aspect ratio case. We use a pair of coupled lines with a separation (gap) of 0.1 µm and a line width of 0.1 µm. The line width is meshed

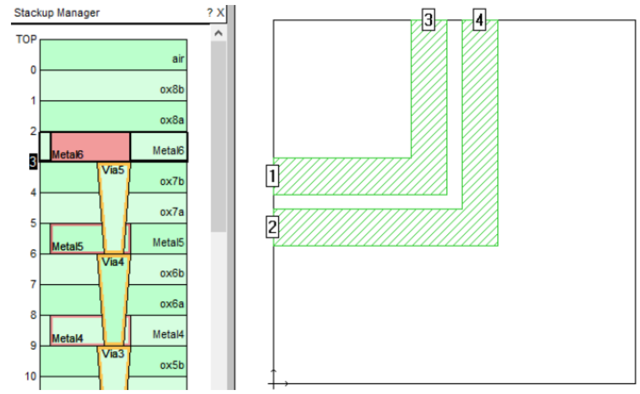

Fig. 3. Stackup and layout for the extremely thick coupled line validation test. A generic stackup is modified by changing Metal 6 to a thickness of 30 µm. The line widths ar 6 µm and the line gap is 2.4 µm. Results and 3-D view of the circuit in Fig. 4..

eight cells wide. The line thickness is 10 µm, 100 times greater than the gap. The line length is 60 µm.

This geometry requires 100 or more sheets to analyze accurately using the multi-sheet model and is not possible with this mesh size and current computer resources. So instead, we compare with a proprietary Sonnet model often used for tightly coupled lines on Si RFIC.

Analysis at all frequencies gives similar results for capacitance per line length. The volume rooftop model (only one layer), gives 298 fF. The validated proprietary model for tightly coupled lines we use for Si RFICs gives 302 fF, confirming the validity of the volume rooftop model for thick metal. A simple parallel plate model of the gap capacitance gives 312 fF. To verify sensitivity to metal thickness, we also analyze the coupled line using the 2-sheet model, resulting in only 10 fF confirming that metal thickness is the dominant factor in this coupled line.

V. Extreme Thickness Validation Test

We have also derived and implemented method of moments coupling between multiple layers of volume rooftop subsections. We did this by evaluating the surface impedance presented to the top and bottom surfaces of the source dielectric layer due to the actual top and bottom cover surface impedances transformed by the cascade of rectangular waveguides formed by the intervening dielectric layers and the conducting sidewalls of the containing box. We may then evaluate the fields in any layer that are due to a source subsection in any other layer.

To validate the multi-layer coupling model, we select a coupled line with a right angle bend to test modeling of thick transmission lines using multiple layers of volume rooftops. For a benchmark, we compare results to our already validated [10] multiple-sheet model. This test circuit is evaluated on a generic Si RFIC stackup, a portion of which is shown in Fig. 3. The line widths are 6 µm and the gap between lines is 2.4 µm. A typical metal thickness would be 3 µm, however, we wish to have substantial sensitivity to the capacitance between the lines for this multi-layer thick metal validation test, so we drastically increase Metal 6 thickness to 30 µm.

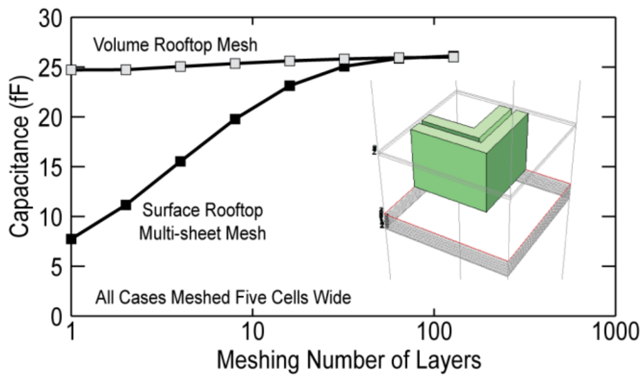

Fig. 4. The volume rooftop subsections provide a nearly converged answer for the interline capacitance even with only one layer. The multi-sheet surface rooftop model requires 33 sheets to realize a similar reduction in error.

The results in Fig. 4 show that a single layer of volume rooftops results in a nearly already converged modeled interline capacitance even though we are using only a single layer of volume rooftops. In contrast, the multi-sheet model does not show similar convergence until the separation between sheets is on the order of gap size, at about $N = 32$. This means, at least for this extreme thickness case, even the single-layer volume rooftop model provides accuracy similar to the multi-sheet model with $N+1$ or 33 sheets. Thus, the single layer volume rooftop model uses 33 times fewer subsections. Since method of moments using direct matrix solve is an N^3 process, the speed increase is substantial.

VI. Additional Results

We have evaluated the full dyadic Green's function. Equations (1) and (2) present only the transverse (*x*- and *y*-directed) fields due to transverse source current. We have also evaluated all fields and method of moments reaction integrals for all pair-wise couplings between surface rooftops, volume rooftops, uniform vias (*z*-directed current), and tapered (current varies from zero at the bottom, to maximum at the top) vias. We have additionally evaluated the method of moments reaction integrals including Ohmic loss. All results have also been fully extended to conductors embedded in uniaxial anisotropic dielectric that has a *z*-directed optical axis. These results will be presented once they are fully validated. Unlike the results presented here, the equations for many of these results show a high level of complexity.

VII. Conclusion

We have provided, for the first time, all information needed for implementation of volume rooftop subsections in a shielded planar method of moments analysis. Thick subsections allow rapid and accurate analysis of thick transmission lines as compared to modeling a thick transmission line with a stack of many infinitely thin sheets. Validation examples illustrate that a very large increase in speed is possible for high accuracy analysis of circuits composed of thick transmission lines.

References

[1] R. F. Harrington, Field Computation by Moment Methods, New York, NY, USA:Macmillan, 1968.

[2] F. Tiezzi, J. R. Mosig, "Analysis of printed antennas with inhomogeneous dielectric bodies," IEEE Antennas and Propagation Society International Symposium, June 2002, Vol. 2, pp. 862–865.

[3] B.C. Usner, K. Sertel, M.A. Carr, J.L. Volakis, "Generalized volume-surface integral equation for modeling inhomogeneities within high contrast composite structures", Antennas and Propagation IEEE Transactions on, vol. 54, no. 1, pp. 68–75, 2006.

[4] J. W. Massey, F. Wei, A. E. Yilmaz, "Mixed basis functions for fast analysis of antennas near voxel-based human models," 2013 USNC-URSI Radio Science Meeting (Joint with AP-S Symposium), July 2013, pg. 100.

[5] K. Konno, Q. Chen, R. J. Burkholder, "Fast Computation of Layered Media Green's Function via Recursive Taylor Expansion", IEEE Antennas and Wireless Propagation Letters, vol. 16, pp. 1048–1051, 2017.

[6] A. W. Glisson and D. R. Wilton, "Simple and efficient numercial methods for problems of electromagnetic radiation and scattering from surfaces," IEEE Trans. Antennas Propagat., vol. AP-28, pp. 593–603, 1980.

[7] J. C. Rautio and R. F. Harrington, "An electromagnetic time-harmonic analysis of shielded microstrip circuits," IEEE Trans. Microwave Theory Tech., vol. MTT-35, pp. 726–730, Aug. 1987.

[8] N. Marcuvitz, Waveguide Handbook, Rad. Lab. Ser., vol. 10, New York: McGraw-Hill, 1951.

[9] Sonnet Suites™, Version 16.52, Sonnet Software, Inc., Syracuse, NY USA.

[10] J. C. Rautio, "An ultrahigh precision benchmark for validation of planar electromagnetic analyses," IEEE Tran. Microwave Theory Tech., Vol. 42, No. 11, pp. 2046–2050, Nov. 1994.